

Design and Experimental Study of an Observer-based Controller for a Three-DOF Four-wire Type Optical Pickup Head

C.-P. Chao, J.-S. Huang, C.-W. Chiu and C.-Y. Shen
*Department of Mechanical Engineering, Chung Yuan Christian University,
Chung-Li, Taiwan 32023, R.O.C.*

Abstract—This study presents a servo scheme synthesized via methods of sliding-mode control and high-gain observer for a newly-designed three degree-of-freedom four-wire-type lens actuator which is installed in the pickups of optical disc drives to perform data-reading. The optical pickup considered herein is a particular one that owns three degrees of freedoms, focusing, tracking and tilting. The virtual work and Lagrange's equation are used to derive the equations of motion. The sliding-mode control design is performed to conduct precision positioning of the objective lens in directions of focusing, tracking and simultaneously annihilate possible tilting for faster data-reading and better accuracy. The full-order high-gain observer is next designed to estimate the velocities of the lens to provide low-noised feedback signals for sliding-mode control. Simulations are carried out to verify the theoretical model and the predicted performance of designed controller and observer. Finally, experiments are conducted to validate effectiveness of the proposed controller/observer scheme.

I. INTRODUCTION

Optical disk drives are widely used as basic data-reading devices for various applications such as CD-ROM, DVD, CDP, LDP, etc. One of key components in the optical disk drive is the optical pickup, which performs data reading via a well-designed optical system installed inside the pickup. Figures 1(a,b) show the structure of a three-axis pickup actuator in four-wire type [1,2] and its schematic view with primary axes. A pickup mainly consists of objective lens, bobbin (the lens holder), wire springs, coils and permanent magnets. Due to the flexibility of these wire springs, the bobbin could be easily in motions as the electro-mechanical forces generated by the electromagnetic interaction between the magnetic field induced by permanent magnets and the currents conducted in four wires and coils. A typical actuator is designed in a particular dimensional and geometric

arrangements of wires, coils and magnets such that the electromagnetic interaction generates two independent actuation control forces, respectively, in the directions of focusing (vertical) and tracking (radial relative to the disk), providing control means on the focusing and tracking motions. In addition to the servo capability in focusing and tracking directions, some researchers recently added a pair of coils to create the servo capability in tilting direction [3-5]. This allows the servo system to suppress unavoidable tilting of the pickup, which is caused by an uneven magnetic fields and motions of the pickup.

With servo hardware ready, the method of sliding-mode control theory [6-7] is applied herein to design a controller that is able to perform simultaneous positioning in three axes via canceling coupled dynamics by synthesized control effort. This sliding-mode controller in practice needs to acquire the on-line feedbacks of not only focusing and tracking motions (the two feedbacks needed by conventional servos) but also tilting ones. As to conventional optical disc drives, only motions of tracking and focusing can be detected by method of differential phase detection (DPD) with four patches of photo diodes installed in the pickup, as shown in Fig. 2(a). To remedy the problem, recent research made possible the detection of the tilting by adding more receiving patches in the photo diodes. Fig 2(b) shows one of the new designs by Doh *et al.* [8], where additional four small patches are used.

Along with the controller is a high-gain observer [9-14] designed to estimate the feedback velocities in the purpose of avoiding high differentiation noise due to computer discretization in implementation. Note that most of the high-gain observers were used to estimate the velocities of the robot [10-12], since the joint velocities are usually measured by velocity tachometers, which are expensive and often contaminated by noises.

II. MATHEMATICAL MODELING

The objective lens in a typical pickup is installed on a foundation structure "bobbin," as shown in Fig. 1(a). Due to specially-designed supporting structure of four parallel wires, the lens/bobbin exhibit motions mainly in the directions of tracking (*Y-axis*) and focusing (*X-axis*). In addition to the motions in X and Y directions, small tilting often occurs

Manuscript received on Oct 15, 2004. The authors are greatly indebted to the National Science Council of R.O.C. for the support of the research through contact no. NSC 92-2212-E-033-001.

Paul C.-P. Chao¹, J.-S. Huang², C.-W. Chiu³ and C.-Y. Shen⁴ are with Department of Mechanical Engineering, Chung Yuan Christian University, Chung-Li 32023 Taiwan, R.O.C. (phone: 886-3-2654310, fax: 886-3-2654310, e-mail: pchao@cycu.edu.tw)

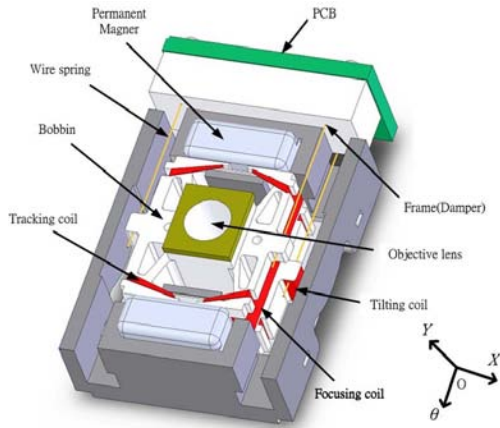


Fig. 1(a) Schematic diagram of a three-axis four-wire type optical pickup.

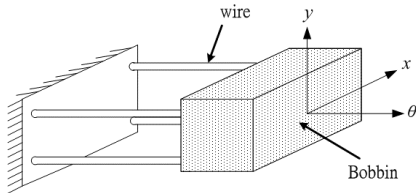


Fig. 1(b) 3D-view of the four-wire type optical pickup.

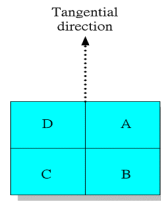


Fig. 2(a) Traditional photo-detector.

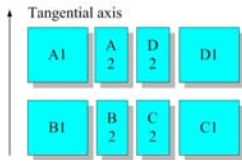


Fig. 2(b) Tilt detection: 8 divided photodiodes.

about (θ -axis), which is caused by manufacturing tolerance, uneven magnetic fields, and geometric mis-passes of the electro-magnetic force acting lines on mass centroids of the bobbin. The objective of this study is to design a controller that owns three independent actuation forces/moment in X, Y and θ directions such that the controller is able to perform precision focusing/tracking and to simultaneously achieve zero tilting to avoid any error in optical signals. Following a standard procedure of formulating kinetic and potential energies and substituting them into Lagrange's equation, one can yield system equation of motion as [16] :

$$\mathbf{M}\ddot{\mathbf{q}} + \mathbf{C}\dot{\mathbf{q}} + \mathbf{K}\mathbf{q} + \mathbf{N} + \mathbf{G} = \bar{\mathbf{T}}\mathbf{V}, \quad (2.1)$$

where $\mathbf{q} = [X \ Y \ \theta]^T$ is the generalized coordinate and \mathbf{V} is the applied voltages. The related detailed expressions are as follows:

$$\mathbf{M} = \begin{bmatrix} \mathbf{m} & 0 & -(\mathbf{I}_x \sin \theta + \mathbf{I}_y \cos \theta) \\ 0 & \mathbf{m} & (\mathbf{I}_x \cos \theta - \mathbf{I}_y \sin \theta) \\ -(\mathbf{I}_x \sin \theta + \mathbf{I}_y \cos \theta) & (\mathbf{I}_x \cos \theta - \mathbf{I}_y \sin \theta) & \mathbf{I}_{\theta\theta} \end{bmatrix},$$

$$\mathbf{K} = \text{diag} [k_x, k_y, k_\theta], \mathbf{V} = [V_x \ V_y \ V_\theta]^T, \mathbf{G} = [0 \ mg \ 0]^T,$$

$$\mathbf{C} = \begin{bmatrix} C_x + \left(\frac{n_x B_x l_x}{R_x} \right) K_{mvs} & 0 & 0 \\ 0 & C_y + \left(\frac{n_y B_y l_y}{R_y} \right) K_{mvs} & 0 \\ 0 & 0 & C_\theta + \left(\frac{n_\theta B_\theta l_\theta}{R_\theta} \right) K_{mvs} \end{bmatrix},$$

$$\mathbf{N} = \begin{bmatrix} -\dot{\theta}^2 (\mathbf{I}_x \cos \theta - \mathbf{I}_y \sin \theta) \\ -\dot{\theta}^2 (\mathbf{I}_x \sin \theta + \mathbf{I}_y \cos \theta) \\ -\dot{X}\dot{\theta} (\mathbf{I}_x \cos \theta - \mathbf{I}_y \sin \theta) + \dot{Y}\dot{\theta} (\mathbf{I}_x \sin \theta + \mathbf{I}_y \cos \theta) \end{bmatrix},$$

$$\bar{\mathbf{T}} = \begin{bmatrix} \cos \theta \cdot \frac{n_x B_x l_x}{R_x} & -\sin \theta \cdot \frac{n_y B_y l_y}{R_y} & 0 \\ \sin \theta \cdot \frac{n_x B_x l_x}{R_x} & \cos \theta \cdot \frac{n_y B_y l_y}{R_y} & 0 \\ 0 & 0 & \frac{n_\theta B_\theta l_\theta}{R_\theta} \end{bmatrix}.$$

where $\mathbf{I}_{\theta\theta}$ is the mass moment of inertia of the bobbin about its centroid and along the z axis, while $\mathbf{I}_x = \int_m x^2 dm$ and $\mathbf{I}_y = \int_m y^2 dm$ are first mass moments of inertia with respect to y and x axes, respectively. k_x , k_y and k_θ are the equivalent spring stiffnesses in tracking, focusing and tilting directions; $n_{(x,y,\theta)}$ is the number of coils; $B_{(x,y,\theta)}$ is the magnetic flux densities within the air gap between bobbin and magnets; $l_{(x,y,\theta)}$ is the effective coil lengths; $R_{(x,y,\theta)}$ is the voice coil's resistance.

III. CONTROLLER DESIGN

With a complete dynamic model in hand, a sliding-mode

controller is next designed in this section for precise positioning of the pickup actuator in 3 DOF's. In the design process, three independent control inputs are synthesized to

reach the control goal, which are tracking, focusing and annihilating tilting. To achieve the aforementioned goals, Eq. (2.1) is first re-written as

$$\ddot{\mathbf{q}} = -\mathbf{M}^{-1}\mathbf{C}\dot{\mathbf{q}} - \mathbf{M}^{-1}\mathbf{K}\mathbf{q} - \mathbf{M}^{-1}\mathbf{D} + \mathbf{M}^{-1}\bar{\mathbf{T}}\mathbf{V}, \quad (3.1)$$

where $\mathbf{D} = (\mathbf{N} + \mathbf{G})$. The control error vector of the system is in fact

$$\mathbf{e} = \mathbf{q} - \mathbf{q}_d = [X - X_d, Y - Y_d, \theta - \theta_d]^T, \quad (3.2)$$

where $\mathbf{q}_d = [X_d, Y_d, \theta_d]^T$ are targeted focusing, tracking and tilting positions. The switching vector $\mathbf{S}(\mathbf{e})$ in an integral form to eliminate steady-state positioning error is defined by

$$\mathbf{S}(\mathbf{e}) = \dot{\mathbf{e}} + 2\mathbf{C}_1\mathbf{e} + \mathbf{C}_1^2 \int_0^t \mathbf{e} dt, \quad (3.3)$$

where $\mathbf{C}_1 = \text{diag}[C_{1x}, C_{1y}, C_{1\theta}]$, a matrix with positive diagonal elements to be determined for different control performances. Incorporating Eqs. (3.1-3.2) into Eq. (3.3) and taking a time derivative on $\mathbf{S}(\mathbf{e})$ give

$$\begin{aligned} \dot{\mathbf{S}} &= (\dot{\mathbf{e}} + 2\mathbf{C}_1\dot{\mathbf{e}} + \mathbf{C}_1^2\mathbf{e}) \\ &= [(-\mathbf{M}^{-1}\mathbf{C}\dot{\mathbf{q}} - \mathbf{M}^{-1}\mathbf{K}\mathbf{q} - \mathbf{M}^{-1}\mathbf{D} + \mathbf{M}^{-1}\bar{\mathbf{T}}\mathbf{V}) - \dot{\mathbf{q}}_d] \\ &\quad + 2\mathbf{C}_1(\dot{\mathbf{q}} - \dot{\mathbf{q}}_d) + \mathbf{C}_1^2(\mathbf{q} - \mathbf{q}_d). \end{aligned} \quad (3.4)$$

To find an appropriate control law, the approach employed herein is first to determine the reaching law of the states with proportional plus switched constant power rate in the form of

$$\dot{\mathbf{S}} = -\mathbf{P}\mathbf{S} - \mathbf{Q} \text{sgn}(\mathbf{S}), \quad (3.5)$$

where $\mathbf{Q} = \mathbf{W} \cdot [|S_x|^\alpha, |S_y|^\alpha, |S_\theta|^\alpha]^T$ with S_x, S_y, S_θ being components of given sliding-mode matrix \mathbf{S} . P and W are positive constant weighting coefficients to be designed, while the choices of α allows one to adjust relative convergence speed in three axes. By selecting appropriate P and \mathbf{Q} in Eq. (3.5), the convergence of state trajectories to the switching surface can be guaranteed if

$$\mathbf{S} \cdot \dot{\mathbf{S}} < \mathbf{0}. \quad (3.6)$$

To accomplish the above goal, the controller \mathbf{V} can be designed as follows based the theory of sliding-mode control.

$$\mathbf{V} = [V_x, V_y, V_\theta]$$

$$= (\mathbf{M}^{-1}\bar{\mathbf{T}})^{-1} \begin{pmatrix} \mathbf{M}^{-1}\mathbf{C}\dot{\mathbf{q}} + \mathbf{M}^{-1}\mathbf{K}\mathbf{q} + \mathbf{M}^{-1}\mathbf{D} + \dot{\mathbf{q}}_d - \mathbf{C}_1\dot{\mathbf{q}} \\ + \mathbf{C}_1\dot{\mathbf{q}}_d - \mathbf{P}\mathbf{S} - \mathbf{Q} \text{sgn}(\mathbf{S}) \\ + (\mathbf{C}_1)^2 \int_0^t (\mathbf{q} - \mathbf{q}_d) dt \end{pmatrix}. \quad (3.8)$$

In order to reduce the chattering near the switching surface, the function $\text{sgn}(\mathbf{S})$ in Eq. (3.5) is replaced by a saturation function inside a designated boundary layer. The saturation function is chosen as

$$\text{sat}(\mathbf{S}) = \begin{cases} \text{sgn}(\mathbf{S}), & \text{if } |\mathbf{S}| > \phi_s \\ \mathbf{S}/\phi_s, & \text{if } |\mathbf{S}| \leq \phi_s \end{cases}, \quad (3.9)$$

where ϕ_s is the boundary layer width of the switching surface.

IV. FULL-ORDER HIGH-GAIN OBSERVER DESIGN

The high-gain observer is designed next in this section to estimate moving velocities of the bobbin/lens, the process of which follows the procedure similar to that in [15]. This starts with defining new state and output variables of the system as $\mathbf{q}_1 = \mathbf{q}$, $\mathbf{q}_2 = \dot{\mathbf{q}}$, and $\mathbf{y} = \mathbf{q}$, respectively. With these new definitions, the system equations (3.1) can be expressed as

$$\begin{aligned} \dot{\mathbf{q}}_1 &= \mathbf{q}_2, \\ \dot{\mathbf{q}}_2 &= f(\mathbf{q}_1, \mathbf{q}_2) + g(\mathbf{q}_1)\mathbf{V}, \\ \mathbf{y} &= \mathbf{q}_1, \end{aligned} \quad (4.1)$$

where

$$\begin{aligned} f(\mathbf{q}_1, \mathbf{q}_2) &= -\mathbf{M}^{-1}\mathbf{C}\mathbf{q}_2 - \mathbf{M}^{-1}\mathbf{K}\mathbf{q}_1 - \mathbf{M}^{-1}(\mathbf{D} + \mathbf{G}), \\ g(\mathbf{q}_1) &= \mathbf{M}^{-1}\bar{\mathbf{T}}. \end{aligned}$$

Moreover, $\mathbf{V} = [V_x, V_y, V_\theta]$ and \mathbf{y} is the output vector capturing the displacements of the bobbin/lens in three DOFs. With the sliding-mode control effort designed in Eq. (3.8), the term \mathbf{V} can be seen as a function of $\{\mathbf{q}_1, \mathbf{q}_2, \mathbf{t}\}$; i.e., $\mathbf{V} = \eta(\mathbf{q}_1, \mathbf{q}_2, \mathbf{t})$. To simplify procedure of designing the observer, the system equations are further represented as

$$\begin{aligned} \dot{\mathbf{q}}_1 &= \mathbf{q}_2, \\ \dot{\mathbf{q}}_2 &= \phi(\mathbf{q}_1, \mathbf{q}_2, \mathbf{t}), \\ \mathbf{y} &= \mathbf{q}_1, \end{aligned} \quad (4.2)$$

where $\phi(\mathbf{q}_1, \mathbf{q}_2, \mathbf{t}) = f(\mathbf{q}_1, \mathbf{q}_2) + g(\mathbf{q}_1)\eta(\mathbf{q}_1, \mathbf{q}_2, \mathbf{t})$. Consider the high-gain observer in form of

$$\begin{aligned} \dot{\hat{\mathbf{q}}}_1 &= \hat{\mathbf{q}}_2 + \frac{1}{\varepsilon} \mathbf{H}_p(\mathbf{y} - \hat{\mathbf{q}}_1), \\ \dot{\hat{\mathbf{q}}}_2 &= \frac{1}{\varepsilon^2} \mathbf{H}_v(\mathbf{y} - \hat{\mathbf{q}}_1), \end{aligned} \quad (4.3)$$

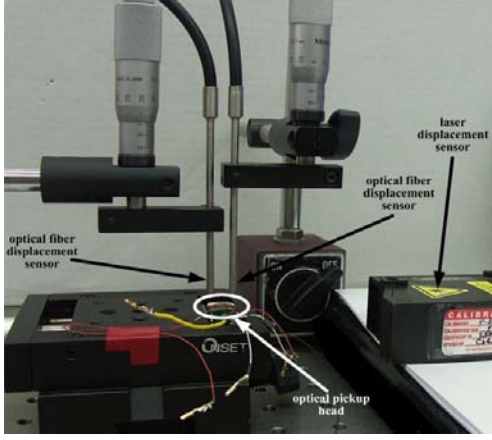


Fig. 3(a) The experiment framework including the optical pickup and three displacement sensors.

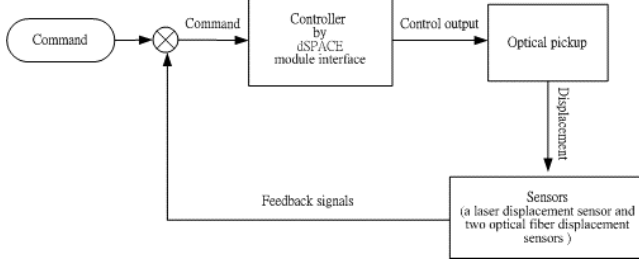


Fig. 3(b) The schematic diagram of experiment.

where $\hat{\mathbf{q}}_1$ and $\hat{\mathbf{q}}_2$ denote, respectively, the estimates on \mathbf{q}_1 and \mathbf{q}_2 , the displacement and velocities of the bobbin/lens. On the other hand, $\mathbf{H}_p = \text{diag}(h_{p,i})$ and $\mathbf{H}_v = \text{diag}(h_{v,i})$ are constant diagonal matrices, which need to be chosen such that the spectra of the characteristic polynomials

$$p_i(\lambda) = \lambda^2 + h_{p,i}\lambda + h_{v,i}, \quad i = 1, \dots, N,$$

are in the left half plane. Finally in Eq. (4.3), ε is a small parameter that results in high observer gains for a satisfactory convergent speed of estimation. The equations governing the error dynamics of estimation by the observer can be obtained by subtracting Eqs. (4.3) from Eqs. (4.2), yielding

$$\begin{aligned} \dot{\tilde{\mathbf{q}}}_1 &= \tilde{\mathbf{q}}_2 - \frac{1}{\varepsilon} \mathbf{H}_p(\tilde{\mathbf{q}}_1), \\ \dot{\tilde{\mathbf{q}}}_2 &= -\frac{1}{\varepsilon^2} \mathbf{H}_v(\tilde{\mathbf{q}}_1) + \phi(\mathbf{q}_1, \mathbf{q}_2, \mathbf{t}), \end{aligned} \quad (4.4)$$

where $\tilde{\mathbf{q}}_i = \mathbf{q}_i - \hat{\mathbf{q}}_i$, $i = 1, 2$. For further analysis, the following new coordinates and scalings are introduced.

$$\tilde{\mathbf{z}}_1 = \tilde{\mathbf{q}}_1, \quad \tilde{\mathbf{z}}_2 = \varepsilon \tilde{\mathbf{q}}_2, \quad \tilde{\mathbf{z}} = (\tilde{\mathbf{z}}_1^T, \tilde{\mathbf{z}}_2^T)^T. \quad (4.5)$$

With the above, the error dynamics in Eq. (4.5) can be expressed as

$$\begin{aligned} \varepsilon \dot{\tilde{\mathbf{z}}}_1 &= -\mathbf{H}_p \tilde{\mathbf{z}}_1 + \tilde{\mathbf{z}}_2, \\ \varepsilon \dot{\tilde{\mathbf{z}}}_2 &= -\mathbf{H}_v \tilde{\mathbf{z}}_1 + \varepsilon^2 \phi(\mathbf{q}_1, \mathbf{q}_2, \mathbf{t}), \end{aligned}$$

or in a matrix form

$$\varepsilon \dot{\tilde{\mathbf{z}}} = \mathbf{A}_o(\tilde{\mathbf{z}}) + \varepsilon^2 \mathbf{b} \phi(\mathbf{q}_1, \mathbf{q}_2, \mathbf{t}), \quad (4.6)$$

where

$$\mathbf{A}_o = \begin{bmatrix} -\mathbf{H}_p & \mathbf{I} \\ -\mathbf{H}_v & \mathbf{0} \end{bmatrix}, \quad \mathbf{b} = \begin{bmatrix} \mathbf{0} \\ \mathbf{I} \end{bmatrix}.$$

Since matrices \mathbf{H}_p and \mathbf{H}_v have been chosen so that spectra of $p_i(\lambda)$, $i = 1, \dots, N$, are in the left half plane, there exists a positive definite matrix \mathbf{P}_o such that $\mathbf{W}(\tilde{\mathbf{z}}) = \tilde{\mathbf{z}}^T \mathbf{P}_o \tilde{\mathbf{z}}$ can serve as a Lyapunov function candidate for the error dynamics in Eq. (4.6). Computing the derivative of $\mathbf{W}(\tilde{\mathbf{z}})$ along the solutions of Eq. (4.6), one obtains

$$\begin{aligned} \frac{d\mathbf{W}}{dt} &= \frac{1}{\varepsilon} [\tilde{\mathbf{z}}^T (\mathbf{A}_o^T \mathbf{P}_o + \mathbf{P}_o \mathbf{A}_o) \tilde{\mathbf{z}} + 2\varepsilon^2 \phi(\mathbf{q}_1, \mathbf{q}_2, \mathbf{t})^T \mathbf{b}^T \mathbf{P}_o \tilde{\mathbf{z}}] \\ &= -\frac{1}{\varepsilon} \tilde{\mathbf{z}}^T \tilde{\mathbf{z}} + 2\varepsilon \phi(\mathbf{q}_1, \mathbf{q}_2, \mathbf{t})^T \mathbf{b}^T \mathbf{P}_o \tilde{\mathbf{z}}. \end{aligned} \quad (4.7)$$

Eq. (4.7) arrives further at

$$\frac{d\mathbf{W}}{dt} \leq -\frac{1}{\varepsilon} \|\tilde{\mathbf{z}}\|^2 + 2\varepsilon \|\mathbf{P}_o \mathbf{b} \phi(\mathbf{q}_1, \mathbf{q}_2, \mathbf{t})\| \|\tilde{\mathbf{z}}\|. \quad (4.8)$$

To ensure convergence of the high-gain observer, one can tune the parameter of ε small enough to satisfy

$$\varepsilon^2 < \frac{\|\tilde{\mathbf{z}}\|}{2\|\mathbf{P}_o \mathbf{b} \phi(\mathbf{q}_1, \mathbf{q}_2, \mathbf{t})\|}. \quad (4.9)$$

Due to the fact that the controlled system renders a finite quantity at R.H.S. of inequality (4.9), there must exist a small value of ε for observer convergence. However, inequality (4.9) also indicates, from another point of view, that with a small finite ε the estimation error $\|\tilde{\mathbf{z}}\|$ by the observer never reaches zero, only contained by a small quantity that satisfies required observer performance. Therefore, in the process of determining ε , one can detune ε from a moderate small value with assistance from simulations until the observer reaches its required convergence speed for controller use.

V. NUMERICAL AND EXPERIMENTAL RESULTS

The previously-proposed controller and observer designs are applied herein to a realistic three-axis optical pickup for

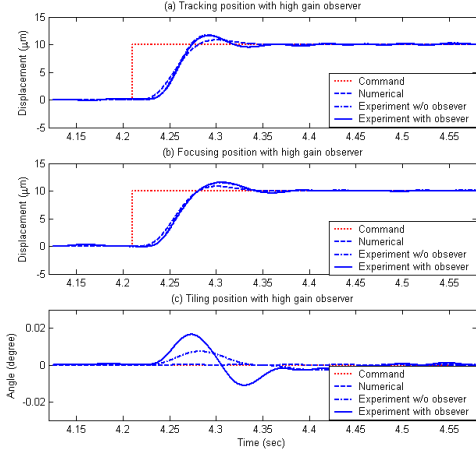


Fig. 4 Responses of a three-axis optical pickup using sliding-mode control assisted by the observer.

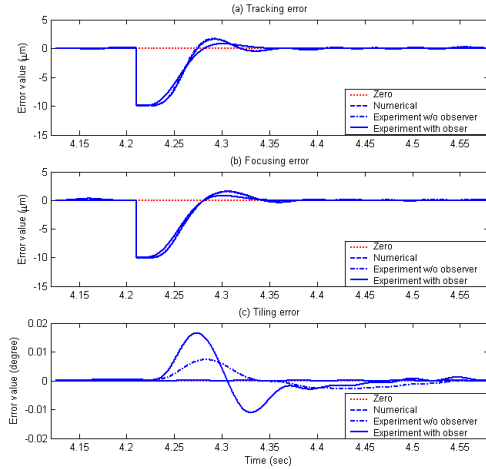


Fig. 5 Position control errors by sliding-mode control of three-axis optical pickup head.

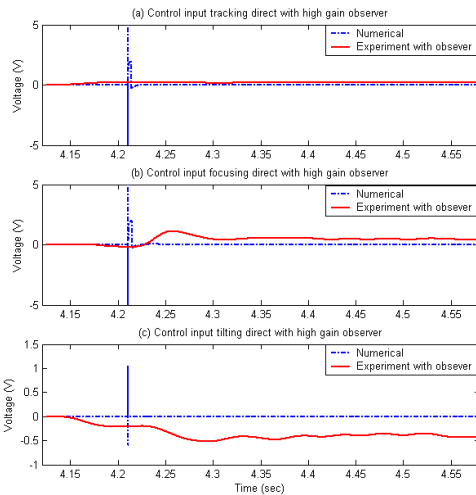


Fig.6 Control effort by sliding-mode control of three-axis optical pickup head.

show the experiment setup in photo and a schematic framework, respectively. The implementation of the control algorithms is accomplished by a dSPACE module. The output control signals of this module are amplified by an OP-741 amplifier circuit to provide driving voltage to move the pickup bobbin/lens in the three-axis pickup head. The motion in three directions of the bobbin/lens are measured by a laser displacement sensor (MTI250) for tracking and two optical fiber displacement sensors (MTI KD-300) for focusing and tilting. The sensor signals are filtered to reduce noise before feedbacked to the dSPACE module for computing output control effort. Note that the resolution of the laser displacement and optical sensors are both around $\pm 0.5 \sim 0.6 \mu m$. Parameters of the three-axis four-wire type optical pickup actuator are identified using various fundamental calibration methods. They are obtained as

$$m = 2.87 \times 10^{-4} \text{ kg}, L = 12.5 \times 10^{-3} \text{ m}$$

$$I = 1.01 \times 10^{-17} \text{ m}^4, E = 1.1 \times 10^{11} \text{ Pa}, r = 4 \times 10^{-5} \text{ m}$$

$$R_x = 4 \times 10^{-3} \text{ m}, R_y = 2.15 \times 10^{-3} \text{ m}, \Delta t = 5 \times 10^{-4} \text{ sec.}$$

The sliding-mode controller and high-gain observer are synthesized following the procedure stated in section III and IV. The gain matrices for the switching function and the designated rate of reaching mode for the controller are chosen as

$$C_1 = \text{diag}[300 \ 300 \ 900], P = 50000, Q = 10.$$

For observer, the small gain of ε is determined to be $\varepsilon = 0.00005$ for a fast estimation. This value of ε is determined from a recursive tuning process on ε based on a number of simulations.

The desired trajectories in X and Y directions are set to be step functions, while the desired tilting in θ direction is set to be zero. The simulated responses and associated errors are shown in Fig. 4 and 5, respectively, while control efforts are shown in Fig. 6. Three different cases are considered; i.e., the one with controller but no observer applied, the one with controller with the observer applied, and the associated numerical one. It is first seen from these figures that the simulated response is close to those experimental counterparts, which confirms the validity of the theoretical model established and identified parameters in this study. It is also generally found from Figs. 4-6 that the experimental cases with or without the observer lead to almost identical responses in three axes, showing satisfactory performance of the high-gain observer. Finally, it is observed that with the tilt servo mechanism provided by the sliding-mode controller, the nonzero tilting in transient stage eventually approaches zero in favor of better data-reading quality.

The experiment without the tilting control mechanism;

validating the predicted performance. Figure 3(a) and (b)

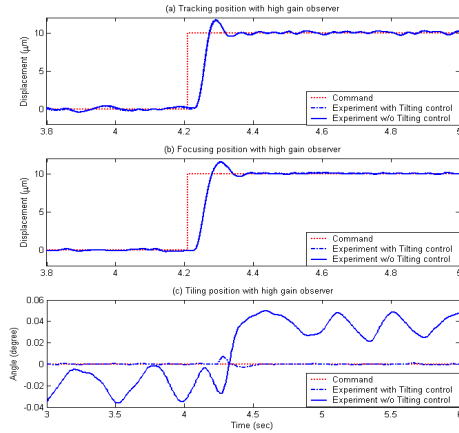


Fig.7 Responses of a three-axis optical pickup using sliding-mode control assisted by the observer with and without tilting control.

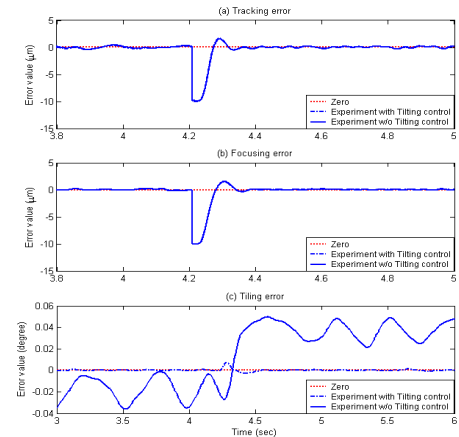


Fig.8 The position control errors of sliding-mode control with high-gain observer providing velocity states feedback with and without tilting control.

i.e., the traditional two-axis control, is also conducted to be compared with the case with current designed frame work of controller/observer. The results are shown in Figs. 7-8 along with the current design, where it is seen that without tilting control, the bobbin/lens eventually converge to a small, nonzero tilting angle, while with the tilting servo applied, no tilting angle is present at steady state.

VI. CONCLUSIONS

A tilting-elimination servo scheme designed via the theory of sliding-mode control is successfully synthesized and incorporated into conventional focusing/tracking mechanism for an optical pickup used in various types of disc drives. With assistance from a designed high-gain observer next, the proposed sliding-mode controller owns implementability. Experiments are conducted in a laboratory to validate the predicted performance of the proposed servo scheme from theoretical study.

The experimental results show that the simultaneous

control of the bobbin/lens in three axes is achieved successfully as opposed to the case of the conventional two-axis control where the tilting angle cannot be reduced to zero at steady state. Furthermore, the experimental and simulated results are very close to each other, showing the validity of the theoretical model established. Finally, the experimental study for the cases with and without observer leads to almost identical responses in three axes, showing satisfactory performance of the high-gain observer.

ACKNOWLEDGMENT

The authors are greatly indebted to the National Science Council of R.O.C. for the support of the research through contact no. NSC 92-2212-E-033-001.

REFERENCES

- [1] Kajiwara and A. Nagamatsu, "Optimum Design of Optical Pick-up by Elimination of Resonance Peaks", *Journal of Vibration and Acoustics* 115, 1993, pp 377-383.
- [2] K. Lim, Y. Lee, S. Kim and J. Lee, "Dynamic Characteristics of Actuator for High-Density Optical Recording Pick-up", *Proceedings of the Korean Society for Noise and Vibration Engineering*, 1995, pp. 258-263.
- [3] S. Lim and T. Y. Jung, "Dynamics and Robust Control of a High Speed Optical Pickup", *Journal of Sound and Vibration*, 4, 1999, pp. 607-621.
- [4] J. Y. Kang and M. G. Yoon, "Robust Control of an Active Tilting Actuator for High-Density Optical Disk", *Proceedings of the American Control Conference*, 1998, pp. 861-865.
- [5] M. Nagasato and I. Hoshino, "Development of Two-Axis Actuator with Small Tilt Angles for One-Piece Optical Head", *Japanese Journal of Applied Physics*, part 1, 35, 1996, pp. 392-397.
- [6] Y. Itkis., *Control System of Variable Structure*, Wiley, New York, 1976.
- [7] V. I. Utkin., *Sliding Modes and Their Applications in Variable Structure System*, Mir, Moscow, 1978.
- [8] Tae-Yong Doh, Byung In Ma, Byoung Ho Choi, In Sik Park, Chong Sam Chung, Yong-Hoon Lee, Seok Jung Kim and Dong Ho Shin, "Radial Tilt Detection Using One Beam and Its Compensation in a High-Density Only Memory", *Japanese Journal of Applied Physics*, part 1, 35, 2001, pp.1680-1683.
- [9] A. Dabroom and H.K. Khalikl, "Numerical Differentiation Using High-Gain Observers", *Proceedings of the 36th Conference on Decision & Control*, 1997, pp. 4790-4795.
- [10] J. A. Heredia and W. Y., "A High-Gain Observer-Based PD Control for Robot Manipulator", *Proceedings of the American Control Conference*, 2000, pp. 2518-2522.
- [11] S. Nicosia, A. Tornambe and P. Valigi, "Experimental results in state estimation of industrial robots", *Proceedings of the 29th Conference on Decision and Control*, 1990, pp. 360-365.
- [12] E. S. Shin and K. W. Lee, "Robust Output Feedback Control of Robot Manipulators Using High-Gain Observer", *Proceedings of the International Conference on Control Applications*, 1999, pp. 881-886.
- [13] H. K. Khalil, "Nonlinear System", Upper Saddle River, N.J. Prentice Hall, Third Edition, 2002.
- [14] A. Isidon, "Nonlinear Control Systems", Berlin, New York, Springer, Third Edition, 1995.
- [15] G. Besancon, "Further Results on High Gain Observers for Nonlinear systems", *Proceedings of the 38th Conference on Decision & Control*, 1999, pp. 2904-2909.
- [16] L. Meirovitch., "Analytical Methods in Vibrations", London: Macmillan, 1967.